Collective estimation of ocean nonlinear internal waves using robotic underwater drifters

Michael Ouimet Jorge Cortés

Abstract

This paper considers a group of drogues whose objective is to estimate the physical parameters that determine the dynamics of ocean nonlinear internal waves. Internal waves are important in oceanography because, as they travel, they are capable of displacing small animals, such as plankton, larvae, and fish. These waves are described by models that employ trigonometric functions parameterized by a set of constants such as amplitude, wavenumber, and temporal frequency. While underwater, individual drogues do not have access to absolute position information and only rely on inter-drogue measurements. Building on this data and the study of the drogue dynamics under the flow induced by the internal wave, we design two strategies, termed the `Vanishing Derivative Method` and the `Passing Wave Method`, that are able to determine the wavenumber and the speed ratio. Either of these strategies can be employed in the `Parameter Determination Strategy` to determine all remaining wave parameters. We analyze the correctness of the proposed strategies and discuss their robustness against different sources of error. Simulations illustrate the algorithm performance under noisy measurements as well as the effect of different initial drogue configurations.

I. Introduction

Internal waves are waves that propagate within a fluid, rather than on its surface. The type that we consider here corresponds to a moving oscillation in the boundary surface between two layers of a stratified fluid. In the ocean, these two layer fluids can occur at the mouth of large rivers where brackish (low salinity) water sits above sea water, for instance. Also, a continuously stratified fluid can be modeled as a two-layer fluid, where the interface, called pycnocline, is

Parts of this paper were submitted in preliminary form to the 2013 IEEE Conference on Decision and Control.

The authors are with the Department of Mechanical and Aerospace Engineering, University of California, San Diego, CA 92093, USA, {miouimet,cortes}@ucsd.edu

the surface of constant density where the vertical rate of change in density is largest. This class of internal waves can be broadly categorized into linear and nonlinear. Linear waves have amplitudes small relative to the depth of the water column. They are capable of moving around plankton, animal larvae, and other organisms, as well as creating mixing between the upper and lower layers. In contrast, nonlinear waves have larger amplitudes, allowing them to be an agent of transport of small oceanic life. Here, we consider nonlinear waves modeled as solitons, which are stable, solitary peaks (or troughs) which propagate along the pycnocline.

Traditional methods for studying internal waves have been satellite observations, acoustic tomography, conductance-temperature-depth (CTD) casts, and current meters on moorings. However, these methods lack the capability of real-time adaptability. Here, we tackle this problem using a group of drogues capable of drifting underwater near the internal wave's interface to determine the physical parameters that define its motion. A drogue is a robotic Lagrangian drifter able to actuate its depth by changing its buoyancy. While underwater, drogues are subject to the flow induced by the motion of the internal wave and do not have access to exact location information. Figure 1 presents a pictorial illustration of the problem setup. The basic premise of the paper is that the evolution of the inter-drogue distance and distance derivative measurements contains enough information for the drogues to be able to fully characterize the internal wave.

Literature review: Internal waves are associated with high concentrations of various types of planktonic organisms and small fishes [2], [3], as well as an agent of larval transport [1]. This makes their study important to oceanographers, see e.g. [4], [5], [6], [7]. In particular, striping of low/high densities in plankton can be well explained by small amplitude, linear internal waves [4]. However, nonlinear waves are needed to account for the advection required for larval transport [1]. Many models exist for nonlinear waves [8], [9] to account for the wide variety of conditions and bathymetries found in the ocean. Scientists widely use drogues drifting passively as monitoring platforms to gather relevant ocean data [10], [11], [12]. The use of autonomous underwater vehicles to detect and characterize internal waves is a relatively new approach. Whereas previous works use ocean measurements such as conductivity, temperature, pressure data [13], [14] or vertical flow velocity [15] to detect and analyze internal waves, our approach is unique in using inter-vehicles measurements. Recent work [16] explores the possibility of actively selecting tidal currents so that drogues can autonomously reach a desired destination. An increasing body of work in the systems and control literature deals with cooperative networks

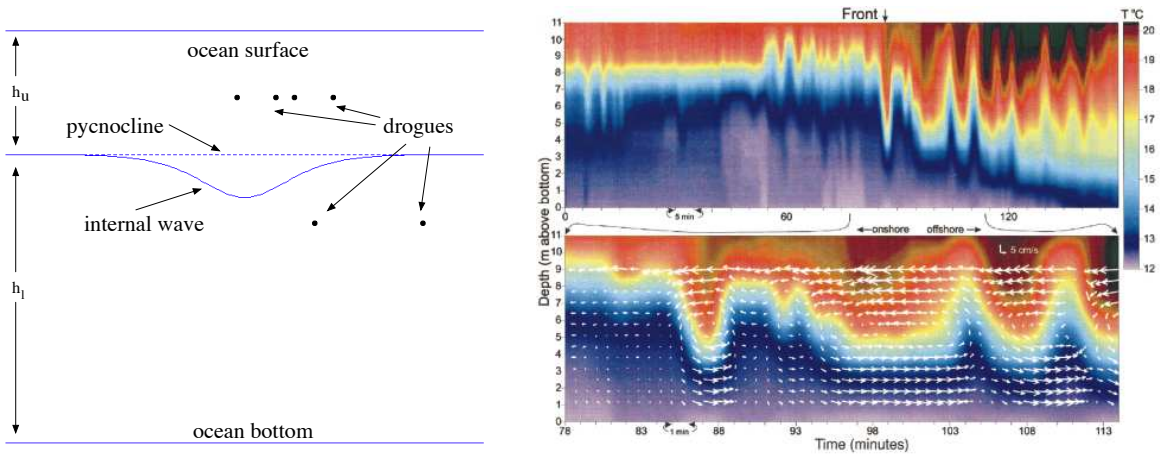

(a) Schematic of drogues and internal wave

(b) Thermal fluctuations induced by an internal wave

Fig. 1. For an ocean nonlinear internal wave, (a) shows its spatial structure at a fixed instant of time whereas (b) shows its temporal structure at a fixed horizontal location. In (a), one can see a vertical cross-section of the ocean perpendicular to the wave propagation direction. A group of drogues float at constant depths (but not necessarily along a straight line) and do not have access to exact location information. Our objective is to provide drogues with mechanisms that rely only on the relative distances between them to determine the parameters that uniquely define the internal wave. In (b), one can see temperature and vertical/onshore-offshore current vectors data taken from a train of nonlinear soliton internal waves about one kilometer off the coast of La Jolla, CA on July 3, 1996. The bottom figure is a zoom-in of the top figure. Figure (b) is © (1999) by the Association for the Sciences of Limnology and Oceanography, Inc., see [1] for additional information.

of agents estimating spatial natural phenomena, including ocean [17], [18], [19], river [20], and hurricane sampling [21]. This work builds off our previous work [22], which considers a similar estimation problem for linear internal waves. The nonlinear wave case considered here presents novel challenges of its own given the complexity and different nature of the induced drogue dynamics.

Statement of contributions: We consider the problem of estimating the physical parameters of a nonlinear internal wave that is propagating horizontally. A group of underwater Lagrangian drifters are subjected to the flow induced by the internal wave and can only measure inter-drogue distances and distance derivatives. Because the drogues only have access to these relative measurements, they must rely on the presence of other drogues to achieve their task. The benefit obtained here by 'the power of many' in the estimation of the ocean flow field is a key feature of our paper. Our first contribution is the establishment of an analytic expression for the dynamic evolution of the drogues. We analyze the asymptotic behavior of the solutions, which

corresponds to the drogue's displacement after the wave has passed. Building on this analysis, and specifically on the observation that when the crest of the wave is exactly at the midpoint between two drogues, their inter-drogue distance derivative becomes zero, we design two strategies for determining the spatial frequency and speed ratio of the wave, which we call the `Vanishing Derivative Method` and the `Passing Wave Method`. Either of these methods are used as a component of the `Parameter Determination Strategy`, an algorithm run on the drogues using only relative measurements which is capable of determining all the wave parameters. We analyze the correctness of these algorithms for the case of noiseless inter-drogue measurements. We discuss the robustness properties of the `Parameter Determination Strategy` to different sources of error such as noise in measurements, finite sampling rate, and model uncertainty, which arise in realistic implementations. Finally, several simulations compare the robustness performance to measurement noise of the `Vanishing Derivative Method` and the `Passing Wave Method`, as well as illustrate the effect of initial drogue locations on the algorithm performance.

Organization: Section II introduces some basic notation used throughout the paper. Section III introduces the internal wave and drogue models, as well as describes the problem statement. Section IV analyzes the dynamics of drifting drogues under the nonlinear internal wave. Section V proposes and analyzes two strategies for determining the wavenumber and speed ratio parameters. Section VI presents the `Parameter Determination Strategy`, analyzes its correctness under noiseless measurements, and discusses its inherent robustness to various sources of errors present in practical implementations. Several simulations illustrate the performance of the algorithm under measurement noise. Finally, Section VII gathers our conclusions and ideas for future work.

II. Notational conventions

Here we present some notational conventions used in the paper. Let $\mathbb{R}$, $\mathbb{R}_{>0}$, and $\mathbb{R}_{\geq 0}$ denote the set of all, positive, and non-negative real numbers, respectively. A reference frame Σ_g in $\mathbb{R}^3$ is composed of an origin $\mathbf{p}_g \in \mathbb{R}^3$ and a set of orthonormal vectors $\{\mathbf{e}_{x_g}, \mathbf{e}_{y_g}, \mathbf{e}_{z_g}\} \subset \mathbb{R}^3$. A point $\mathbf{q}$ and a vector $\mathbf{v}$ can be uniquely expressed with respect to the frame Σ_g and are denoted by $\mathbf{q}^g$ and $\mathbf{v}^g$, respectively. Next, let $\Sigma_b = (\mathbf{p}_b, \{\mathbf{e}_{x_b}, \mathbf{e}_{y_b}, \mathbf{e}_{z_b}\})$ be a reference frame fixed to a moving body. The origin of Σ_b is a point $\mathbf{p}_b$, denoted as $\mathbf{p}_b^g$ when expressed with respect to Σ_g.

The orientation of Σ_b is characterized by the rotation matrix Q_b^g whose columns are the vectors $\{\mathbf{e}_{x_b}, \mathbf{e}_{y_b}, \mathbf{e}_{z_b}\}$ expressed with respect to Σ_g. With this notation, a change of reference frame is given by

$$\mathbf{q}^g = Q_b^g \mathbf{q}^b + \mathbf{p}_b^g, \quad \mathbf{v}^g = Q_b^g \mathbf{v}^b.$$

Finally, the Euclidean norm of vector $\mathbf{v}$ is $\|\mathbf{v}\|$.

III. Problem statement

This section contains the nonlinear internal wave model used, the model for the drogue drifters and their interaction with the internal wave, and a formalized problem statement.

A. Nonlinear internal wave model

Let $\Sigma_g = (\mathbf{p}_g, \{\mathbf{e}_{x_g}, \mathbf{e}_{y_g}, \mathbf{e}_{z_g}\})$ be a global reference frame defined as follows: the origin p_g corresponds to an arbitrary point at the ocean surface; the vector $\mathbf{e}_{x_g}$ corresponds to the direction of wave propagation, which is parallel to the ocean bottom, and $\mathbf{e}_{z_g}$ is perpendicular to the ocean bottom, pointing from bottom to surface. For convenience, the coordinates induced by Σ_g are denoted by $\{x, y, z\}$.

As shown in Figure 1, an internal wave is a wave with travels beneath the surface of the ocean, along a surface of constant water density called a pycnocline. When the amplitude of the wave becomes a large enough fraction of the water column, the wave begins to 'feel' the surface and bottom of the ocean and nonlinear terms of the governing PDE must be included. One classical equation used to model weakly nonlinear long internal waves is the Korteweg-de Vries (KdV) equation, see e.g., [9]:

$$\frac{\partial \eta}{\partial t} - \frac{3}{2} c \frac{h_l - h_u}{h_u h_l} \eta \frac{\partial \eta}{\partial x} + \frac{1}{6} c h_u h_l \frac{\partial^3 \eta}{\partial x^3} = 0, \tag{1}$$

where η is the distance that the internal wave is displacing the pycnocline, $c = \sqrt{g \frac{|\rho_l - S\rho_u|}{\rho_l} \frac{h_u h_l}{h_u + h_l}}$, ρ_u, h_u and ρ_l, h_l are the density and depth of the upper and lower layers, respectively, and g is the acceleration due to gravity. In the absence of an internal wave, the pycnocline is at depth h_u. The stable soliton solution to (1) is, cf. [8],

$$\eta(x,t) = -\frac{2Ch_u h_l}{h_l - h_u} \operatorname{sech}^2 \left(\frac{1}{2} \sqrt{\frac{6C}{c h_u h_l}} (x - Ct - \chi_0) \right) = A \operatorname{sech}^2 \big(k(x - \chi_0) - \omega t \big),$$

where

$$A = -\frac{2Ch_u h_l}{h_l - h_u} \quad k = \frac{1}{2}\sqrt{\frac{6C}{ch_u h_l}}, \quad \omega = \frac{1}{2}\sqrt{\frac{6C}{ch_u h_l}}C,$$

are wavenumber and temporal frequency, respectively, $C = \frac{\omega}{k}$ is the celerity (speed) of the wave, and χ_0 is the initial location of the center of the wave. As the wave propagates, it induces motion in the nearby water. The standard model assumes that the vertical velocity varies linearly with depth. Coupled with the conservation of mass law for an incompressible fluid, one can derive the following expressions for the horizontal u_u and vertical v_u velocities of the upper layer

$$\begin{aligned} u_u(x,t) &= -\frac{2CA}{h_u}\operatorname{sech}^2(k(x-\chi_0)-\omega t), \\ v_u(x,z,t) &= \frac{2\omega A z}{h_u}\operatorname{sech}^2(k(x-\chi_0)-\omega t)\tanh(k(x-\chi_0)-\omega t). \end{aligned}$$

Likewise, the horizontal u_l and vertical v_l velocities of the lower layer are

$$\begin{aligned} u_l(x,t) &= \frac{2CA}{h_l}\operatorname{sech}^2(k(x-\chi_0)-\omega t), \\ v_l(x,z,t) &= 2\omega A\frac{h_u+h_l-z}{h_l}\operatorname{sech}^2(k(x-\chi_0)-\omega t)\tanh(k(x-\chi_0)-\omega t). \end{aligned}$$

For convenience, we define the upper and lower velocity amplitudes as $B_u = -\frac{2CA}{h_u}$ and $B_l = \frac{2CA}{h_l}$.

Remark III.1 *(Bounds on wave parameters)* We assume that, for each wave parameter, there exists a closed and bounded interval in $\mathbb{R}_{>0}$ that the parameter is guaranteed to fall within. This is reasonable because natural parameters, such as an object's size or speed, cannot be arbitrarily small or large. We refer to a parameter's bounds with subscripts min and max. •

B. Drogue model

A drogue is a submersible buoy which can drift in the ocean, unattached to the ocean floor or a boat, and is able to change its depth in the water by controlling its buoyancy. While underwater, a drogue can measure the relative distance, distance derivative, and orientation in space to other drogues through sensing (e.g., via acoustic or optical sensors and an onboard compass). A drogue can also measure its depth. However, it does not have access to absolute position because GPS is unavailable underwater.

Consider a group of N drogues, each with a reference frame $\Sigma_i = (\mathbf{p}_i, \{\mathbf{e}_{x_i}, \mathbf{e}_{y_i}, \mathbf{e}_{z_i}\})$, $i \in \{1, \ldots, N\}$, attached to it. The origin $\mathbf{p}_i$ corresponds to the location of the drogue. As in the global coordinate frame Σ_g, $\mathbf{e}_{z_i}$ is perpendicular to the ocean bottom, pointing from bottom to surface. The vectors $\mathbf{e}_{x_i}$ and $\mathbf{e}_{y_i}$ are parallel to the ocean floor, but neither is necessarily oriented in the direction of wave propagation. Thus, each drogue i must determine the angle between $\mathbf{e}_{x_i}$ and $\mathbf{e}_x$, which we denote by θ_i. We assume that each drogue maintains its own prescribed depth by means of buoyancy control. Drogue i senses inter-drogue measurements with the M closest drogue neighbors. Then, for each neighbor j, drogue i has access to

$$\mathbf{d}_{i,j} = (d_{i,j}^{x_i}, d_{i,j}^{y_i}, d_{i,j}^{z_i}) = \mathbf{x}_j - \mathbf{x}_j,$$
$$\dot{\mathbf{d}}_{i,j} = (\dot{d}_{i,j}^{x_i}, \dot{d}_{i,j}^{y_i}, 0) = \dot{\mathbf{x}}_j - \dot{\mathbf{x}}_j.$$

Drogue i actually measures $\|\mathbf{d}_{i,j}\|$ and $\|\dot{\mathbf{d}}_{i,j}\|$ and then uses the relative orientation sensing to decompose the measurements into their components. For now, we assume the drogues have continuous access to these quantities. Later in Section VI, we elaborate on the fact that a large enough, finite sampling rate will produce parameter estimates which are unique and remain close to the true values.

We make the simplifying assumption that the drogues' dynamics are Lagrangian, i.e., the drogue's velocity is equal to ocean's velocity at its current location. Thus, without loss of generality, the dynamics of drogue $i \in \{1, \ldots, N\}$ in the upper layer is

$$\dot{\mathbf{p}}_i = (\dot{x}_i, \dot{y}_i, \dot{z}_i) = (u_u(x,t), 0, 0)$$

and can be similarly defined for drogues in the lower layer.

Remark III.2 *(Kinematic versus dynamical model)* The Lagrangian dynamics is a simplification of the second-order dynamical model, see e.g. [23],

$$m\ddot{x} = -c_d\,|\dot{x} - u_{\mathrm{u}}(t,x)|(\dot{x} - u_{\mathrm{u}}(t,x)), \tag{2a}$$

$$\dot{y} = 0, \tag{2b}$$

$$m\ddot{z} = -c_d\,|\dot{z} - w_{\mathrm{u}}(t,x,z)|(\dot{z} - w_{\mathrm{u}}(t,x,z)) + f, \tag{2c}$$

where m denotes the combined drogue mass and inertial added mass [24], c_d is the drag parameter, and f is the buoyancy control input. Following [4], [12], reasonable values for

wave/ocean parameters are $h_u = 10$ m, $h_l = 60$ m, $C = .1\frac{\text{m}}{\text{s}}$, and $\frac{|\rho_l - \rho_u|}{\rho_l} = .002$ and drogue parameters are $m = 1.5$kg, and $c_d = 210\frac{\text{Ns}^2}{m^2}$. Figure 2 depicts the position, inter-drogue distance, and velocity evolution for a pair of drogues initially at rest 50 m and 55 m from the crest of the internal wave. In these simulations, the spatial wavelength is about 250 m. In Figure 2(a), one can see that the Lagrangian model approximates well the second-order one, with the drogue's position error on the order of .1 m. In Figure 2(b), one can see that since drogues are close relative to the spatial wavelength, their position errors are roughly the same, causing the errors in distance to be of the order .01 m. This comparison provides a good justification for the use of the simpler Lagrangian model. In Section VI, we revisit the effect of this approximation when discussing the sources of errors present in realistic implementations. •

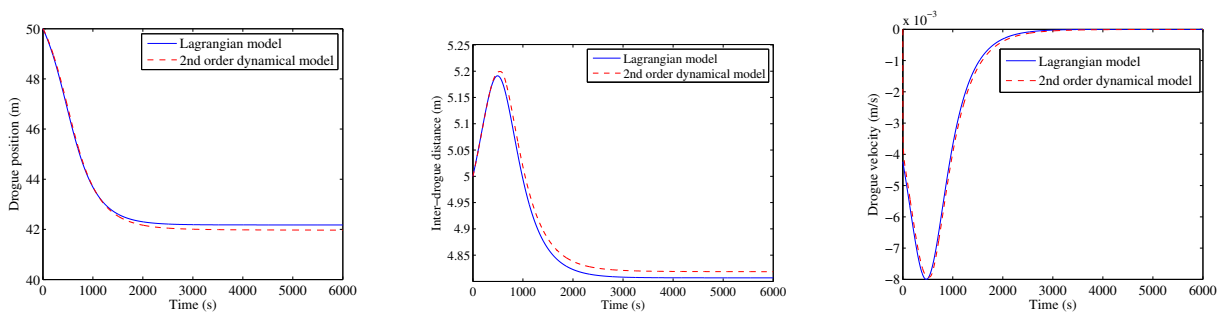

(a) Position evolution (b) Inter-drogue distance evolution (c) Velocity evolution

Fig. 2. The plots show the position, inter-drogue distance, and velocity evolution for the Lagrangian and second-order dynamical models. The closeness of the two models justifies the use of the simpler Lagrangian model. The wave/ocean parameters are $h_u = 10$ m, $h_l = 60$ m, $C = .1\frac{\text{m}}{\text{s}}$, and $\frac{|\rho_l - \rho_u|}{\rho_l} = .002$ (implying a spatial wavelength of about 250 m) and the drogue parameters are $m = 1.5$kg, and $c_d = 210\frac{\text{Ns}^2}{m^2}$

C. Problem description

A team of N drogues is deployed in the ocean and their motion is governed by an internal wave. The drogues may control their depth through buoyancy changes, and each one can measure the relative distance and orientation to the closest M drogues in their own coordinate frame. Our objective is to design an algorithm that allows the drogues to collectively determine the physical parameters C, $\frac{|\rho_u - \rho_l|}{\rho_l}$, h_u, and h_l which define the internal wave.

IV. Analysis of Lagrangian drifter motion driven by nonlinear internal wave

In this section, we outline a method for the drogues to determine the direction that the internal wave is propagating and derive equations for the motion of a depth-keeping drogue under the influence of a nonlinear internal wave. Both of these are key ingredients for the ensuing discussion.

A. Determining the wave propagation direction

The first task a drogue must solve is to determine the direction in which the wave is propagating. For completeness, we briefly review here the method presented in our previous work [22] to enable a drogue $i \in \{1, \ldots, N\}$ to determine θ_i, the angle difference between the wave propagation direction and its own local coordinate system.

For drogues undergoing motion purely caused by an internal wave, inter-drogue distances in their local reference frame can be projected onto the global reference frame $\mathbf{d}^g_{i,j} = Q^g_i \mathbf{d}_{i,j}$ via the transformation matrix Q^g_i,

$$Q^g_i = \begin{bmatrix} \cos\theta_i & -\sin\theta_i & 0 \\ \sin\theta_i & \cos\theta_i & 0 \\ 0 & 0 & 1 \end{bmatrix}.$$

The global coordinate frame is useful because the inter-drogue distance in the e_y direction is constant, i.e., $\dot{d}^y_{i,j} = 0$. Since θ_i is constant, it can be found using the measurements available, $\dot{d}^y_{i,j} = \dot{d}^{x_i}_{i,j} \sin\theta_i + \dot{d}^{y_i}_{i,j} \cos\theta_i = 0$, and hence

$$\theta_i = \tan^{-1}\left(-\dot{d}^{y_i}_{i,j} / \dot{d}^{x_i}_{i,j}\right).$$

Once drogues know θ_i, they can project all measurements onto the wave propagation direction, where all the dynamics are occurring. Thus, to ease the presentation, we employ the simplified notation $d_{i,j}$ to denote $d^x_{i,j}$ from now on.

B. Analyzing the motion of the Lagrangian drifter

Here, we analyze the dynamics of a depth-maintaining drogue that moves under the influence of an internal wave. We begin by defining the speed ratio

$$D = \sqrt{\left|\frac{B}{B-C}\right|},$$

which measures the ratio of the maximum water velocity to the difference between the wave velocity and maximum water velocity. The following result describes the drogue's trajectory in implicit form.

Lemma IV.1 *(Implicit expression of the drogue trajectory) Let $B \in \mathbb{R}$, $k, \omega \in \mathbb{R}_{>0}$, and $t_0 \in \mathbb{R}_{\geq 0}$. The solution of*

$$\dot{x} = B \operatorname{sech}^2(k(x - \chi_0) - \omega t),$$

starting at time t_0 can be implicitly described by

$$D\Big(\tan^{-1}\Big(D \tanh(k(x(t) - \chi_0) - \omega t)\Big) - \tan^{-1}\Big(D \tanh(k(x(t_0) - \chi_0) - \omega t_0)\Big)\Big) = -k(x(t) - x(t_0)), \quad (3)$$

if $0 < kB < \omega$ and otherwise by

$$D\Big(\tanh^{-1}\Big(D \tanh(k(x(t) - \chi_0) - \omega t)\Big) - \tanh^{-1}\Big(D \tanh(k(x(t_0) - \chi_0) - \omega t_0)\Big)\Big) = k(x(t) - x(t_0)). \quad (4)$$

Proof: Let $z = k(x - \chi_0) - \omega t$. In this new coordinate, the dynamics can be expressed as

$$\dot{z} = kB \operatorname{sech}^2(z) - \omega.$$

Integrating both sides,

$$\int_{z_0}^{z} \frac{d\beta}{kB \operatorname{sech}^2(\beta) - \omega} = \int_{t_0}^{t} d\tau.$$

yields

$$D \tanh^{-1}\Big(D \tanh(z)\Big) - D \tanh^{-1}\Big(D \tanh(z_0)\Big) + z_0 - z = \omega(t - t_0).$$

The second case follows from substituting the definition of z. From there, the first case follows from the identity that $\sqrt{-1} \tanh^{-1}(\sqrt{-1} f(x)) = -\tan^{-1}(f(x))$. ■

From Section III-A, note that the sign of B is different for the upper and lower layer, and the sign that each takes is dependent on the relative ocean layer thicknesses. Consequently the form of the drogue trajectory is dependent on whether the drogue is in the upper or lower layer as well as on the sign of $h_u - h_l$. For the rest of this section, we assume that the drogues are

in the ocean layer which makes B negative. Similar results hold in the opposite case which we omit for the sake of clarity.

At most times, the position of the wave relative to the drogues is unknown. However, at times when inter-drogue distance derivatives momentarily vanish, one can gain insight as the following result shows.

Lemma IV.2 *(Relative wave position when distance derivative vanishes) For two drogues i and j at initial positions $x_i(t_0) \neq x_j(t_0)$, if $x_i(t_0)$, $x_j(t_0) > \chi_0$, then there exists time $t_{\mathrm{cr}} > 0$ when $\dot{d}_{i,j}(t_{\mathrm{cr}}) = 0$ and*

$$k\Big(\frac{x_j(t_{\mathrm{cr}}) + x_i(t_{\mathrm{cr}})}{2} - \chi_0\Big) = \omega t_{\mathrm{cr}}. \tag{5}$$

Proof: The proof follows from noticing that the inter-drogue distance derivative is zero when the crest of the wave is exactly between the two drogues. Since the drogue's maximum speed is less than the wave's constant speed, this can happen at most one time. The condition that $x_i(t_0)$, $x_j(t_0) > \chi_0$ ensures that it has not happened yet, but will. One determines (5) by solving for the arguments that make inter-drogue distance derivative equal to zero, excluding the degenerate case that the drogues are coincident. ■

Since absolute position information is unavailable, the following result expands on Lemmas IV.1 and IV.2 to only use inter-drogue distance information.

Corollary IV.3 *(Change in inter-drogue distance after wave passes) For any drogues i, j and $B < 0$, the following holds*

$$d_{i,j}(\infty) - d_{i,j}(t_{\mathrm{cr}}) = -\frac{2D}{k}\tanh^{-1}\big(D\tanh(k\frac{d_{i,j}(t_{\mathrm{cr}})}{2})\big). \tag{6}$$

Proof: Note that for any $x_i(t_0)$ finite, $x_i(\infty)$ is finite, as well. Letting $t_0 = t_{\mathrm{cr}}$, $t = \infty$ in (4), and applying (5) one gets the following equation for drogue i:

$$D\Big(\tanh^{-1}\big(-D\big) - \tanh^{-1}\big(D\tanh(\frac{-kd_{i,j}(t_{\mathrm{cr}})}{2})\big)\Big) = k(x_i(\infty) - x_i(t_{\mathrm{cr}})). \tag{7}$$

One can create a similar equation to (7) for drogue j. Subtracting the two yields the result. ■

V. Strategies to determine the wavenumber and speed ratio

In this section, we introduce two methods to determine the spatial wavenumber k and the speed ratio D. Both methods rely on the same rationale which we informally describe next.

> *[Informal description of rationale]: Our strategies for determining the physical parameters which define the internal wave are based on first determining the phase of the wave relative to the drogues at some time. In general, one cannot detect the phase: however, our methods leverage the fact that, when the crest of the wave is exactly between two drogues, their inter-drogue distance derivative becomes zero. When this happens, the drogues can determine the phase. Using this insight, one can create equations between inter-drogue measurements and the parameters of interest. The crux of the analysis is to ensure that only the true set of parameters solve the constructed set of equations.*

Before introducing the algorithms, we briefly mention an assumption on the drogue locations that simplifies the presentation. The algorithms are written for a generic drogue which requires inter-drogue measurements with respect to other agents, and we assume that they all are in the ocean layer where the flow amplitude B is negative (which itself depends on the relative layer thicknesses).

A. Vanishing derivative method

The first method, called the `Vanishing Derivative Method`, requires the capability for measuring both inter-drogue distance and its derivative. It is written in terms of drogue i using measured inter-drogue data between itself and nearest neighbors with identities j_1, j_2, and j_3.

From the Lagrangian drogue model, the dynamics of an inter-drogue distance between drogues i and j in the wave propagation direction is described by

$$\dot{d}_{i,j} = B(\operatorname{sech}^2(k(x_j - \chi_0) - \omega t) - \operatorname{sech}^2(k(x_i - \chi_0) - \omega t)).$$

Note that B, k, χ_0, and ω are all unknown parameters. However, using Lemma IV.2 to write the ratio of two of the above equations for i, j_2 and i, j_3, specifically at the time t_{cr} when

$\dot{d}_{i,j_1}(t_{\rm cr}) = 0$, one gets

$$\frac{\dot{d}_{i,j_2}}{\dot{d}_{i,j_3}} - \frac{\operatorname{sech}^2(k(d_{i,j_2} - \frac{d_{i,j_1}}{2})) - \operatorname{sech}^2(k\frac{d_{i,j_1}}{2})}{\operatorname{sech}^2(k(d_{i,j_3} - \frac{d_{i,j_1}}{2})) - \operatorname{sech}^2(k\frac{d_{i,j_1}}{2})} = 0,$$

which becomes a function only of the unknown parameter k. We now wish to show that only the true value of k satisfies this equation. With this in mind, we define the function f as

$$\mathrm{f}(\mathcal{k}, d_{i,j_1}, d_{i,j_2}, d_{i,j_3}, \dot{d}_{i,j_2}, \dot{d}_{i,j_3}) = \frac{\dot{d}_{i,j_2}}{\dot{d}_{i,j_3}} - \frac{\operatorname{sech}^2(\mathcal{k}(d_{i,j_2} - \frac{d_{i,j_1}}{2})) - \operatorname{sech}^2(\mathcal{k}\frac{d_{i,j_1}}{2})}{\operatorname{sech}^2(\mathcal{k}(d_{i,j_3} - \frac{d_{i,j_1}}{2})) - \operatorname{sech}^2(\mathcal{k}\frac{d_{i,j_1}}{2})}. \tag{8}$$

The next result examines the number of roots of f.

Lemma V.1 *(Uniqueness of spatial wavenumber) Given noiseless measurements of* $d_{i,j}(t_{\rm cr})$*, for* $j \in \{j_1, j_2, j_3\}$*, and of* $\dot{d}_{i,j}(t_{\rm cr})$ *for* $j \in \{j_2, j_3\}$*, where* $t_{\rm cr}$ *is the time when* $\dot{d}_{i,j_1}(t_{\rm cr}) = 0$*, if* $d_{i,j_1}(t_{\rm cr})$ *is sufficiently small, then* $\mathcal{k} = k$ *is the only root to* (8)*.*

Proof: Note that when $d_{i,j_1} = 0$, f reduces to

$$\tilde{\mathrm{f}}(\mathcal{k}, d_{i,j_2}, d_{i,j_3}, \dot{d}_{i,j_2}, \dot{d}_{i,j_3}) = \mathrm{f}(\mathcal{k}, 0, d_{i,j_2}, d_{i,j_3}, \dot{d}_{i,j_2}, \dot{d}_{i,j_3}) = \frac{\dot{d}_{i,j_2}}{\dot{d}_{i,j_3}} - \frac{\operatorname{sech}^2(\mathcal{k}(d_{i,j_2})) - 1}{\operatorname{sech}^2(\mathcal{k}(d_{i,j_3})) - 1}.$$

Showing that $\frac{\partial \tilde{\mathrm{f}}}{\partial \mathcal{k}}$ is either strictly positive or strictly negative ensures that only $\mathcal{k} = k$ is a root of (8). Note that

$$\frac{\partial \tilde{\mathrm{f}}}{\partial \mathcal{k}} = \tanh(\mathcal{k} d_{i,j_2}) \operatorname{sech}^2(\mathcal{k} d_{i,j_2}) \coth(\mathcal{k} d_{i,j_3}) \cdot \operatorname{csch}^2(\mathcal{k} d_{i,j_3})(d_{i,j_2} \sinh(2\mathcal{k} d_{i,j_3}) - d_{i,j_3} \sinh(2\mathcal{k} d_{i,j_2})),$$

is strictly positive if $d_{i,j_2} < d_{i,j_3}$ and strictly negative if $d_{i,j_2} > d_{i,j_3}$, for all $\mathcal{k} > 0$. This shows that $\mathcal{k} = k$ is the unique root of (8) when $d_{i,j_1}(t_{\rm cr}) = 0$. By continuity of $\frac{\partial \mathrm{f}}{\partial \mathcal{k}}$, for $d_{i,j_1}(t_{\rm cr})$ close enough to 0, the above argument guarantees that $\frac{\partial \mathrm{f}}{\partial \mathcal{k}}$ is either strictly positive or strictly negative (depending on the sign of $d_{i,j_2} - d_{i,j_3}$), which completes the result. ■

This result ensures that one can find k by determining the root of (8). Once k has been determined, we wish leverage it to calculate other parameters. Building on (6), we define g as follows,

$$\mathrm{g}(\mathcal{k}, \mathcal{D}, d_{i,j_1}(t_{\rm cr}), d_{i,j_1}(\infty)) = d_{i,j_1}(\infty) - d_{i,j_1}(t_{\rm cr}) + \frac{2\mathcal{D}}{\mathcal{k}} \tanh^{-1}\left(\mathcal{D} \tanh(\mathcal{k}\frac{d_{i,j_1}(t_{\rm cr})}{2})\right). \tag{9}$$

The next result states that given knowledge of k, one can solve for D using the function g. Its proof follows from noting that g is increasing in $\mathcal{D}$.

Lemma V.2 *(Uniqueness of speed ratio) Given noiseless measurements of k, $d_{i,j_1}(t_{\rm cr})$, and $d_{i,j_1}(\infty)$, where $t_{\rm cr}$ is such that $\dot{d}_{i,j_1}(t_{\rm cr}) = 0$, then $\mathcal{D} = D$ is the only root to* (9).

Algorithm 1 `Vanishing Derivative Method`

1: Set $t_{\rm cr}$ such that $\dot{d}_{i,j_1}(t_{\rm cr}) = 0$

2: k uniquely solves $\mathrm{f}(\mathcal{k}, d_{i,j_1}(t_{\rm cr}), d_{i,j_2}(t_{\rm cr}), d_{i,j_3}(t_{\rm cr}), \dot{d}_{i,j_2}(t_{\rm cr}), \dot{d}_{i,j_3}(t_{\rm cr})) = 0$

3: D uniquely solves $\mathrm{g}(\mathcal{D}, k, d_{i,j_1}(t_{\rm cr}), d_{i,j_1}(\infty)) = 0$

Based on the above discussion, we present formally the `Vanishing Derivative Method` as Algorithm 1. The following result, whose proof follows from Lemmas V.1 and V.2, states its correctness.

Proposition V.3 *(Correctness of `Vanishing Derivative Method`) Given $d_{i,j}(t_{\rm cr})$, for $j \in \{j_1, j_2, j_3\}$, $d_{i,j_1}(\infty)$, and $\dot{d}_{i,j}(t_{\rm cr})$, for $j \in \{j_2, j_3\}$, with $d_{i,j_1}(t_{\rm cr})$ sufficiently small and $t_{\rm cr}$ satisfying $\dot{d}_{i,j_1}(t_{\rm cr}) = 0$, then `Vanishing Derivative Method` determines k and D.*

Note that Steps 3 and 4 can be solved using a variety of root-finding methods. Since f and g are monotonic functions, a gradient descent method, for example, would suffice.

B. Passing wave method

This section defines another method for determining the wave's spatial wavenumber and speed ratio. It requires inter-drogue distance measurements and the ability to detect when a distance derivative is zero, but does not need distance derivative values, unlike the `Vanishing Derivative Method`. It is written in terms of drogue i using measured inter-drogue data between itself and drogues j_1 and j_2.

Equation (9) contains 2 unknowns: k and D. It is unclear how many $(\mathcal{k}, \mathcal{D})$ roots there are to two equations of that form. With this in mind, the next result transforms those equations into a more easily analyzable form.

Lemma V.4 *(1-1 correspondence for change of variables) Let $t_{\rm cr,1}$ and $t_{\rm cr,2}$ be the times when $\dot{d}_{i,j_1}(t_{\rm cr,1}) = 0$ and $\dot{d}_{i,j_2}(t_{\rm cr,2}) = 0$, respectively. For $k \in \mathbb{R}_{>0}$, $0 < D < 1$ and measurements*

$d_{i,j_1}(t_{\mathrm{cr},1}), d_{i,j_1}(\infty), d_{i,j_2}(t_{\mathrm{cr},2}), d_{i,j_2}(\infty)$, *the* (k, D) *pairs which solve*

$$2D\tanh^{-1}\left(D\tanh(k\frac{d_{i,j_1}(t_{\mathrm{cr},1})}{2})\right) + k(d_{i,j_1}(\infty) - d_{i,j_1}(t_{\mathrm{cr},1})) = 0, \tag{10a}$$

$$2D\tanh^{-1}\left(D\tanh(k\frac{d_{i,j_2}(t_{\mathrm{cr},2})}{2})\right) + k(d_{i,j_2}(\infty) - d_{i,j_2}(t_{\mathrm{cr},2})) = 0. \tag{10b}$$

have a $1-1$ *correspondence to the* (X, Y) *roots of*

$$X\tanh(X) - YR_1\tanh(Y) = 0, \tag{11a}$$

$$X\tanh(R_2X) - YR_1\tanh(R_3Y) = 0, \tag{11b}$$

where

$$R_1 = \frac{d_{i,j_1}(t_{\mathrm{cr},1})}{d_{i,j_1}(t_{\mathrm{cr},1}) - d_{i,j_1}(\infty)}, \quad R_2 = \frac{d_{i,j_2}(t_{\mathrm{cr},2})}{d_{i,j_1}(t_{\mathrm{cr},1})}, \quad R_3 = \frac{d_{i,j_2}(t_{\mathrm{cr},2}) - d_{i,j_2}(\infty)}{d_{i,j_1}(t_{\mathrm{cr},1}) - d_{i,j_1}(\infty)}.$$

The correspondence is defined by $X = k\frac{d_{i,j_1}(t_{\mathrm{cr},1})}{2}$ *and* $Y = \frac{k}{2D}(d_{i,j_1}(t_{\mathrm{cr},1}) - d_{i,j_1}(\infty))$.

Proof: We begin using trigonometric identities to put (10) into a more palatable form. Noting that

$$\tanh(A+B) = \frac{\tanh(A) + \tanh(B)}{1 + \tanh(A)\tanh(B)},$$

(10) is equivalent to

$$\frac{D\tanh\left(k\frac{d_{i,j_1}(t_{\mathrm{cr},1})}{2}\right) + \tanh\left(\frac{k}{2D}(d_{i,j_1}(\infty) - d_{i,j_1}(t_{\mathrm{cr},1}))\right)}{1 + D\tanh\left(k\frac{d_{i,j_1}(t_{\mathrm{cr},1})}{2}\right)\tanh\left(\frac{k}{2D}(d_{i,j_1}(\infty) - d_{i,j_1}(t_{\mathrm{cr},1}))\right)} = 0,$$

$$\frac{D\tanh\left(k\frac{d_{i,j_2}(t_{\mathrm{cr},2})}{2}\right) + \tanh\left(\frac{k}{2D}(d_{i,j_2}(\infty) - d_{i,j_2}(t_{\mathrm{cr},2}))\right)}{1 + D\tanh\left(k\frac{d_{i,j_2}(t_{\mathrm{cr},2})}{2}\right)\tanh\left(\frac{k}{2D}(d_{i,j_2}(\infty) - d_{i,j_2}(t_{\mathrm{cr},2}))\right)} = 0.$$

Since $0 < D < 1$, the denominators of these equations are strictly positive and hence its roots are the same as those of

$$D\tanh\left(k\frac{d_{i,j_1}(t_{\mathrm{cr},1})}{2}\right) - \tanh\left(\frac{k}{2D}(d_{i,j_1}(t_{\mathrm{cr},1}) - d_{i,j_1}(\infty))\right) = 0, \tag{13a}$$

$$D\tanh\left(k\frac{d_{i,j_2}(t_{\mathrm{cr},2})}{2}\right) - \tanh\left(\frac{k}{2D}(d_{i,j_2}(t_{\mathrm{cr},2}) - d_{i,j_2}(\infty))\right) = 0. \tag{13b}$$

The result follows by substituting for X and Y and noting that the (k, D) to (X, Y) transformation is $1-1$ for $k, D > 0$. ■

The next result identifies conditions for when there exists one unique solution to (11).

Lemma V.5 *(Uniqueness for small Y) For fixed $R_1 > 1$, $R_3^3 > R_2 > R_3 > 1$ and for a small enough interval in Y, there exists at most one pair (X, Y) which solves* (11).

Proof: For each equation of (11), there exists a positive implicit function for X as a function of Y, which we term $\mathbf{X}_1$ and $\mathbf{X}_2$. Since $\mathbf{X}_1$ and $\mathbf{X}_2$ are only implicitly defined, we determine a Taylor series expansion around $Y = 0$. Given that $\mathbf{X}_1$ corresponds to $\mathbf{X}_2$ with $R_2 = R_3 = 1$, we consider the Taylor series approximation of $\mathbf{X}_2$,

$$\mathbf{X}_2(Y) = a_1 Y + a_2 Y^2 + a_3 Y^3 + a_5 Y^5 + \mathcal{O}(Y^7), \tag{14}$$

where

$$a_1 = \sqrt{\frac{R_1 R_3}{R_2}}, \qquad a_2 = 0, \qquad a_3 = \frac{R_3}{6}\sqrt{\frac{R_1 R_3}{R_2}}(R_1 R_2 - R_3).$$

A sufficient condition to guarantee the existence of at most one unique solution pair (X, Y) is that $\frac{d^2 \mathbf{X}_2 - \mathbf{X}_1}{dY^2} > 0$. Looking at the third order expansion of $\mathbf{X}_2 - \mathbf{X}_1$,

$$\mathbf{X}_2(Y) - \mathbf{X}_1(Y) = \Big(\sqrt{\frac{R_1 R_3}{R_2}} - \sqrt{R_1}\Big)Y + \Big(\frac{R_3}{6}\sqrt{\frac{R_1 R_3}{R_2}}(R_1 R_2 - R_3) - \frac{1}{6}\sqrt{R_1}(R_1 - 1)\Big)Y^3,$$

one can see $\mathbf{X}_2 - \mathbf{X}_1$ is convex for small Y, given the assumptions on R_1, R_2, and R_3, which completes the result. ■

Algorithm 2 `Passing Wave Method`

1: Let $t_{\mathrm{cr},1}$ such that $\dot{d}_{i,j_1}(t_{\mathrm{cr},1}) = 0$
2: Let $t_{\mathrm{cr},2}$ such that $\dot{d}_{i,j_2}(t_{\mathrm{cr},2}) = 0$
3: Set $R_1 = \frac{d_{i,j_1}(t_{\mathrm{cr},1})}{d_{i,j_1}(t_{\mathrm{cr},1}) - d_{i,j_1}(\infty)}$, $R_2 = \frac{d_{i,j_2}(t_{\mathrm{cr},2})}{d_{i,j_1}(t_{\mathrm{cr},1})}$, and $R_3 = \frac{d_{i,j_2}(t_{\mathrm{cr},2}) - d_{i,j_2}(\infty)}{d_{i,j_1}(t_{\mathrm{cr},1}) - d_{i,j_1}(\infty)}$
4: Solve for the unique (X, Y) that satisfies

$$X \tanh(X) + Y R_1 \tanh(Y) = 0,$$

$$X \tanh(R_2 X) + Y R_1 \tanh(R_3 Y) = 0.$$

5: Set $k = \frac{2X}{d_{i,j_1}(t_{\mathrm{cr},1})}$
6: Set $D = \frac{k}{2Y}(d_{i,j_1}(t_{\mathrm{cr},1}) - d_{i,j_1}(\infty))$

Based on the above discussion, we present formally the `Passing Wave Method` as Algorithm 2. The following remark provides a justification for its design rationale.

Remark V.6 *(Justification for `Passing Wave Method`)* From Lemma V.4, given knowledge of $d_{i,j_1}(t_{\mathrm{cr},1}) - d_{i,j_1}(\infty)$, one must only search for roots to (11) in the Y interval of $[0, \frac{k_{\max}}{D_{\min}} d_{i,j_1}(t_{\mathrm{cr},1}) - d_{i,j_1}(\infty)]$. By controlling where the drogues are deployed, one has approximate control over $d_{i,j_1}(t_{\mathrm{cr},1})$, and therefore $d_{i,j_1}(t_{\mathrm{cr},1}) - d_{i,j_1}(\infty)$. By Lemma V.5, for small enough Y and fixed coefficients R_1, R_2, and R_3 there exists a unique (X, Y). Thus a reasonable to strategy is to choose $d_{i,j_1}(t_{\mathrm{cr},1})$ small so that the true (X, Y) root is within the range where there is at most one root. However, the coefficients R_1, R_2, and R_3 are themselves functions of $d_{i,j_1}(t_{\mathrm{cr},1})$, and so one cannot easily guarantee that the true root is in the range of at most one root. Nevertheless, simulations appear to show that there is always one unique root. •

VI. Parameter Determination Strategy

This section introduces the `Parameter Determination Strategy` to allow the drogues to find all the physical parameters of the internal wave. Our algorithm design builds on the strategies presented in Section V to determine the wavenumber and the speed ratio. The strategy is formally presented in Algorithm 3. We recall the assumption that drogues i, j_1, j_2, and j_3 are in the ocean layer that makes the flow amplitude B negative as well as introduce an additional one that at least one drogue is in the lower layer and one is in the upper layer. For concreteness we label these drogues as j_4 and j_5, respectively. These assumptions help make the presentation of the algorithm concrete.

The following result establishes the correctness of the algorithm. Its proof follows from the discussion in Section V, as well as the form of the inter-drogue distance derivative equation, and algebraic relations between parameters in the nonlinear soliton model in Section III-A.

Proposition VI.1 *(Correctness of `Parameter Determination Strategy`) Given noiseless knowledge of k and D from either `Vanishing Derivative Method` or `Passing Wave Method`, $d_{i,j}(t_{\mathrm{cr}})$ for $j \in \{j_1, j_2, j_3, j_4\}$, $\dot{d}_{i,j}(t_{\mathrm{cr}})$ for $j \in \{j_2, j_3\}$, the `Parameter Determination Strategy` determines all the internal wave physical parameters.*

Having established the correctness of the algorithm under perfect measurements, let us briefly comment on its performance when errors are present. The fact that all the functions that appear in the equations employed in Algorithms 1-3 have a continuous dependence on the variables makes the `Parameter Determination Strategy` naturally robust against errors, in the

Algorithm 3 `Parameter Determination Strategy`

Set $\theta_i = \tan^{-1}\left(-\dot{d}^{y_i}_{i,j_1}/\dot{d}^{x_i}_{i,j_1}\right)$

Use either Algorithm 1 or 2 to determine k and D

Let t_{cr} such that $\dot{d}_{i,j_1}(t_{\text{cr}}) = 0$

Set $B_l = \frac{\dot{d}_{i,j_4}(t_{\text{cr}})}{\text{sech}^2(k(d_{i,j_4}(t_{\text{cr}}) - \frac{d_{i,j_1}(t_{\text{cr}})}{2})) - \text{sech}^2(k\frac{d_{i,j_1}(t_{\text{cr}})}{2})}$

Set $B_u = \frac{\dot{d}_{i,j_5}(t_{\text{cr}}) + B_l\,\text{sech}^2(k\frac{d_{i,j_1}(t_{\text{cr}})}{2})}{\text{sech}^2(k(d_{i,j_5}(t_{\text{cr}}) - \frac{d_{i,j_1}(t_{\text{cr}})}{2}))}$

Set $\omega = kB_l(1 - \frac{1}{D^2})$

Set $C = \frac{\omega}{k}$

Set $h_u = \frac{h_{\text{ocean}}}{1 - \frac{B_u}{B_l}}$

Set $h_l = h_{\text{ocean}} - h_u$

Set $c = \frac{3C}{2k^2 h_u h_l}$

Set $\frac{|\rho_l - \rho_u|}{\rho_l} = \frac{c^2 h_{\text{ocean}}}{g h_u h_l}$

sense that the estimated parameters are still unique and remain close to the true parameters for small enough errors. For completeness, we discuss the sources of error that arise in practical implementations of the algorithm.

Noise in measurements: In practice one can expect noise in the measurements collected from sensors. We assume that this noise is unbiased, additive, and Gaussian with variance proportional to the measured quantities, and that the noise at different time instances and for different measurements are uncorrelated.

Measurements at $t = \infty$: The proposed algorithm requires knowledge of inter-drogue distances after the wave has completely passed by, i.e., nominally at $t = \infty$. However, in practice one only needs to wait until the wave is sufficiently far away. For instance, when the distance between the drogue and the crest of the wave is 5 spatial wavelengths apart, the effect of the wave is reduced to .02% of its maximum. Not waiting until $t = \infty$ induces a non-random error in the measurements.

Finite sampling: The algorithm assumes measurements at the exact time when the wave is situated exactly between two drogues. However, with finite sampling, the measurements will never be taken at the correct moment, which can be viewed as a nonrandom error in

them. A large enough but finite sampling rate would still allow the algorithm to compute parameter estimates.

Model uncertainty: The problem setup described in Section III-B assumes that drogues are Lagrangian. In practice, drogues have a finite mass and drag coefficient making them not perfectly Lagrangian, leading to a difference between the actual drogue's velocity and the ocean velocity. One can treat this mismatch as an unknown but nonrandom error in the measurements of inter-drogue distances and distance derivatives.

Drogues not maintaining depth: We assume that the drogues have a controller that uses feedback on depth measurements to maintain a desired depth. Due to noisy depth measurements and a desire to minimize actuation cost, instead we assume that the drogues will be within an interval around the desired depth. Although depth is not directly used by the proposed algorithm, this inaccuracy affects inter-drogue distance measurements. As above, one can treat this as an unknown but nonrandom error in the inter-drogue distance measurements.

As noted above, the `Parameter Determination Strategy` is robust against these sources of error independently of their random or deterministic nature. Figure 3 illustrates in simulation this robustness. Figure 3(a) compares the relative error in estimates of the wavenumber k as a function of the relative errors in the inter-drogue distance and its derivative measurements for the `Vanishing Derivative Method` and the `Passing Wave Method`. Note that both methods have a polynomial relationship between relative errors in measurements and relative errors in the wavenumber. However, the `Vanishing Derivative Method` is significantly more robust. Figure 3(b) investigates the effect that the largest inter-drogue distance has in the execution of the `Vanishing Derivative Method`. Three drogues are located at 0, 1, and 2 meters and the fourth drogue's position varies; in three trials it is located at 10, 100, and 200 meters. One can see that as the largest inter-drogue distance grows, the algorithm robustness improves. It is also worth noticing that these plots are the results of a single drogue's estimation of the wavenumber from one set of measurements. Drogues could instead aggregate individual estimates, as well as use multiple sets of data from many different waves, to improve estimates of the parameters.

Figure 4 depicts an actual Lagrangian drogue trajectory along with trajectories generated from the parameters estimated from the `Vanishing Derivative Method` with measurement error of 1% and $.1\%$. As the error in measurements decreases, the algorithm estimates the wave

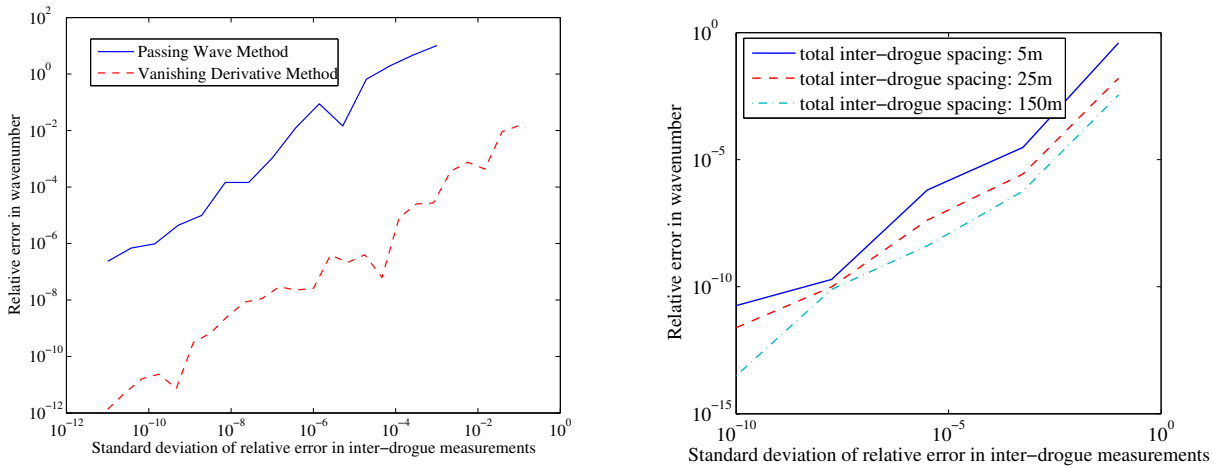

(a) Comparison of methods for determining wavenumber

(b) Effect of inter-drogue spacings on relative error

Fig. 3. (a) plots the relative error in estimates of the spatial wavenumber as a function of the relative errors in the inter-drogue distance and its derivative measurements for the for the `Vanishing Derivative Method` and the `Passing Wave Method`. The true value of the wavenumber is $k = .0178\frac{1}{m}$ and the four drogues were located at 0, 1, 2, and 10 meters from the origin. Each point plotted is the average of 500 runs. Both methods have a polynomial relationship between relative errors in measurements and relative errors in the spatial wavenumber, however, the `Vanishing Derivative Method` is significantly more robust. (b) shows the effect of changing the largest inter-drogue distance on the performance of `Vanishing Derivative Method`. The true value of the wavenumber is $k = .0178\frac{1}{m}$ and the first three drogues were always located at 0, 1, 2 meters. The fourth drogue was at 5, 25, and 150 meters. Here, each point is the average of 2000 runs. One can see that as the largest inter-drogue distance grows, the robustness improves.

parameters more accurately, which produces trajectories closer to the true trajectory. The spatial wavelength $\frac{2\pi}{k}$ in this case is about 290 m, and therefore, the trajectory errors relative to the wave's scale is really small.

VII. Conclusions

We have considered the problem of estimating the physical parameters of a horizontally-propagating nonlinear internal wave. Because of the lack of absolute position information, a group of underwater drogues subject to the flow induced by the internal wave only have access to relative measurements (inter-drogue distances and distance derivatives) with respect to each other to achieve their task. We began by establishing an analytic expression for the dynamic evolution of the drogues and their inter-drogue distances. This analysis set the basis for the design of two strategies, termed `Vanishing Derivative Method` and `Passing Wave`

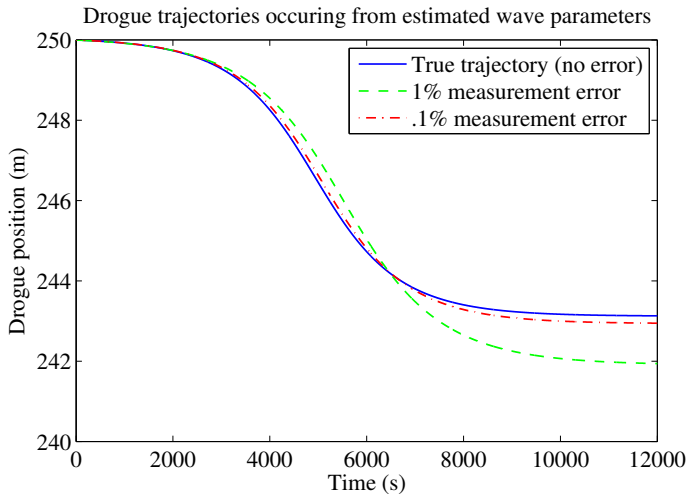

Fig. 4. True Lagrangian drogue trajectory and two trajectories generated from using the parameters estimated by the `Vanishing Derivative Method` with 1% and $.1\%$ measurement error. As the measurement error decreases, the trajectories more closely match the true one. The wave/ocean parameters used are $h_u = 10$ m, $h_l = 60$ m, $C = .05\frac{\text{m}}{\text{s}}$, and $\frac{|\rho_l - \rho_u|}{\rho_l} = .002$.

`Method`, which determine the wavenumber and speed ratio of the wave. Either of these methods can be used by the `Parameter Determination Strategy` to determine all the wave parameters. We analyzed the correctness of these strategies and discussed their robustness against several sources of error arising in realistic implementations. Finally, several simulations have illustrated the algorithmic performance of the two methods under noisy measurements, as well as investigated the effect of initial drogue locations. We have several ideas for future work. The first is to include analytic results regarding the robustness of the algorithm. For instance, it is conceivable that a scheme for aggregating many noisy parameter estimates could be designed to reduce the effect of noise and produce better results. Another line of work is the extension to scenarios involving multiple nonlinear waves whose parameters are unknown. More generally, we plan to explore the design of distributed coordination algorithms run on sensing Lagrangian drifters to study ocean phenomena.

REFERENCES

[1] J. Pineda, "Circulation and larval distribution in internal tidal bore warm fronts," *Limnology and Oceanography*, vol. 44, no. 6, pp. 1400–1414, 1999.

[2] J. R. Zeldis and J. B. Jillett, "Aggregation of pelagic Mundia gregana (Fabncius) (Decapoda, Anomura) by coastal fronts and internal waves," *Journal of Plankton Research*, vol. 4, no. 4, pp. 839–857, 1982.

[3] A. L. Shanks, "Surface slicks associated with tidally forced internal waves may transport pelagic larvae of benthic invertebrates and fishes shoreward," *Marine Ecology Progress Series*, vol. 13, pp. 311–315, 1983.

[4] P. Franks, "Spatial patterns in dense algal blooms," *Limnology and Oceanography*, vol. 42, no. 5, pp. 1297–1305, 1997.

[5] C. Lennert-Cody and P. Franks, "Plankton patchiness in high-frequency internal waves," *Marine Ecology Progress Series*, vol. 18, pp. 59–66, 1999.

[6] R. Susanto, L. Mitnik, and Q. Zheng, "Ocean internal waves observed in the Lombok Strait," *Oceanography*, vol. 18, no. 4, pp. 80–87, 2005.

[7] J. Colosi, R. Beardsley, J. Lynch, G. Gawarkiewicz, C. Chiu, and A. Scotti, "Observations of nonlinear internal waves on the outer New England continental shelf during the summer Shelfbreak Primer study," *Journal of Geophysical Research*, vol. 106, pp. 9587–9601, May 2001.

[8] S. Hamdi, B. Morse, B. Halphen, and W. Scheisser, "Analytical solutions of long nonlinear internal waves: Part I," *Natural Hazards*, vol. 57, no. 3, pp. 597–607, 2011.

[9] K. Helfrich and W. Melville, "Long nonlinear internal waves," *Annual Review of Fluid Mechanics*, vol. 38, pp. 395–425, Jan. 2006.

[10] M. Perry and D. Rudnick, "Observing the ocean with autonomous and Lagrangian platforms and sensors," *Oceanography*, vol. 16, no. 4, pp. 31–36, 2003.

[11] H. J. Freeland and P. F. Cummins, "Argo: A new tool for environmental monitoring and assessment of the world's oceans, and example from the N.E. Pacific," *Progress in Oceanography*, vol. 64, no. 1, pp. 31–44, 2005.

[12] Y. Han, R. A. de Callafon, J. Cortés, and J. Jaffe, "Dynamic modeling and pneumatic switching control of a submersible drogue," in *International Conference on Informatics in Control, Automation and Robotics*, vol. 2, (Funchal, Madeira, Portugal), pp. 89–97, June 2010.

[13] F. Cazenave, "Internal waves over the continental shelf in South Monterey Bay," Master's thesis, San Jose State University, San Jose, CA, USA, 2008.

[14] S. Petillo and H. Schmidt, "Exploiting adaptive and collaborative AUV autonomy for detection and characterization of internal waves," *IEEE Journal of Oceanic Engineering*, 2013. To appear.

[15] Y. Zhang, A. B. Baggeroer, and J. G. Bellingham, "Spectral-feature classification of oceanographic processes using an autonomous underwater vehicle," *IEEE Journal of Oceanic Engineering*, vol. 26, no. 4, pp. 726–741, 2001.

[16] J. Jouffroy, Q. Zhou, and O. Zielinski, "Towards selective tidal-stream transport for Lagrangian profilers," in *Oceans*, (Waikoloa, HI), Sept. 2011.

[17] N. E. Leonard, D. Paley, F. Lekien, R. Sepulchre, D. M. Fratantoni, and R. Davis, "Collective motion, sensor networks, and ocean sampling," *Proceedings of the IEEE*, vol. 45, no. 1, pp. 48–74, 2007. Special Issue on Networked Control Systems.

[18] D. Paley, F. Zhang, and N. Leonard, "Cooperative control for ocean sampling: the glider coordinated control system," *IEEE Transactions on Control Systems Technology*, vol. 16, no. 4, pp. 735–744, 2008.

[19] R. Graham and J. Cortés, "Adaptive information collection by robotic sensor networks for spatial estimation," *IEEE Transactions on Automatic Control*, vol. 57, no. 6, pp. 1404–1419, 2012.

[20] Y. Ru and S. Martínez, "Coverage control in constant flow environments based on a mixed energy-time metric," *Automatica*, 2012. Submitted.

[21] L. DeVries and D. Paley, "Multi-vehicle control in a strong flowfield with application to hurricane sampling," *AIAA Journal of Guidance, Control, and Dynamics*, vol. 35, no. 3, pp. 794–806, 2012.

[22] M. Ouimet and J. Cortés, "Distributed estimation of internal wave parameters via inter-drogue distances," in *IEEE Conf. on Decision and Control*, (Maui, Hawaii), pp. 2433–2438, 2012.

[23] C. Woolsey, "Vehicle dynamics in currents," Technical Report 2011-01, Virginia Polytechnic Institute & State University, Blacksburg,VA, Sept. 2011.

[24] C. Brennen, "A review of added mass and fluid inertial forces," tech. rep., Naval Civil Engineering Laboratory, 1982.